Bulgarian Chemical Communications, Volume 47, Special issue C (pp. 125–132) 2015

A DFT study of CO adsorption and dissociation over γ-$Mo_2N(111)$ plane

S. F. Zaman[1,2]

[1]*Chemical and Materials Engineering Department, Faculty of Engineering, King Abdulaziz University, P.O. Box 80204, Jeddah 21589, Saudi Arabia*
[2]*SABIC Chair of Catalysis, Chemical and Materials Engineering Department, Faculty of Engineering, King Abdulaziz University, P.O. Box 80204, Jeddah 21589, Saudi Arabia*

Received: 9 October 2015; Revised: 23 November 2015

A theoretical investigation of CO dissociation energy barrier over γ-$Mo_2N(111)$ plane has been performed using density functional theory. CO dissociation energy possesses a high activation barrier of 67.96 $kcal.mol^{-1}$ with an endothermic heat of reaction of 28.87 $kcal.mol^{-1}$, starting with CO molecularly adsorbed on a 3-fold hollow fcc site with an adsorption energy of 35.98 $kcal.mol^{-1}$. The activation barrier is little less, 53.03 $kcal.mol^{-1}$, when CO is molecularly adsorbed on a 3-fold hollow hcp site with an adsorption energy of 34.34 $kcal.mol^{-1}$. For both cases, the C-O bond dissociation process is kinetically unfavourable over the investigated surface. A pronounced electronic effect of ligand nitrogen (N) and underlying molybdenum (Mo) layer during bond formation at the surface was observed.

Keywords: CO adsorption, γ-Mo_2N, activation energy, CO dissociation energy.

INTRODUCTION

Density functional theory (DFT) is a quantum chemical computational technique, which solves Schrödinger equation to find the minimum energy state of a system comprising a small number of atoms. This computational tool has been successfully used in the field of heterogeneous catalysis, for example studies of catalyst surface electronic properties and adsorption energies of reactant and products, elementary surface reaction steps of potential surface reaction pathways, etc. [1]. In combination with results of catalyst characterization techniques and catalytic tests, theoretical studies at atomic or molecular scale may provide valuable information about intermediate surface compounds formed on catalyst surfaces and their participation in different steps of the reaction mechanism. This computational tool can be very useful in terms of catalyst screening prior to spending time in the research lab for a desired reaction. In addition, it will give valuable information on the electronic behaviour of the surface and performance of the existing catalyst.

Syngas ($CO+H_2$) conversion to higher hydrocarbons (Fischer-Tropsch synthesis) and mixed alcohol synthesis is a well-established technology. Fischer-Tropsch synthesis (FTS) is been commercialized in several countries to produce middle distillate products, raw materials for various chemicals, and waxes which undergo further cracking to low carbon chain fuels [2]. Recently researchers are looking into the conversion of syngas to higher alcohols (HAS), especially C_2 alcohols, which is another contemporary important research area for clean and alternative transportation fuel production and value added raw material for olefin synthesis. A considerable progress has been achieved in recent years in the development of more active, selective, and stable catalysts for these processes. Important characteristics of the reaction mechanism have been revealed. A dependence of technological parameters of FTS on physical and chemical catalyst properties has also been established [2]. Carbon monoxide is a key reagent in FTS and HAS processes. Numerous studies of the reaction mechanism have shown that the non-dissociative adsorption of CO on the catalyst surface is the first step of the reaction mechanism of both the FTS and HAS processes on supported metal catalysts.

Intensive research activities nowadays are devoted to search for new, highly active, and selective catalytic systems for FTS and HAS processes. An indispensable part of these efforts is studying of surface elementary steps of reaction mechanisms by theoretical methods. One of the key issues that should be revealed for each new catalyst system is information on the mechanism of CO participation in the reaction. Since the adsorption of carbon monoxide is the first step of its activation, it is very important to understand how CO predominantly is adsorbed on a catalyst active surface and what type of surface complexes are being formed.

Because dissociative CO adsorption is leading to formation of coke precursors and active oxygen, this

---

* To whom all correspondence should be sent:
E-mail: zfsharif@gmail.com; sfzaman@kau.edu.sa

reaction route should be depressed by selecting catalyst components, on which the CO is adsorbed non-dissociatively. As an effective criterion for such a discrimination, one can use the energy of CO dissociative adsorption on a particular component. Low energy dissociative adsorption would mean that this component is not a suitable catalyst for FTS and HAS processes. At the same time, the energy of CO adsorption can be used as a criterion of the CO hydrogenation ability of a particular metal [3]. Thus, one has to be capable to exclude such components beforehand by suggesting a suitable criterion.

Molybdenum-based catalysts possess a high hydrogenation ability and have been used by many authors as effective catalysts for FTS and HAS from syngas [4–6]. Addition of p orbital ligands to Mo reduces the CO adsorption energies following the sequence Mo > MoP > γ-MoC > δ-MoN [7]. The energies of CO dissociative adsorption on MoS_2 and Mo_2C have been reported earlier [8,9]. The K-MoS_2 system is a well-known catalyst able to produce ethanol from syngas with high selectivity up to 40% [10], whereas Mo_2C shows a much lower ethanol selectivity [11]. γ-Mo_2N has been used for different reactions, i.e. CO oxidation, HDN, HDO, NH_3 decomposition, etc. and reported for its high activity [12–15], and, in this connection, it may possess some interesting characteristics for CO hydrogenation reactions.

In this study, we report adsorption and dissociation energies of CO over the γ-$Mo_2N(111)$ plane calculated by using DFT. We have set our focus on finding a preferable adsorption arrangement of CO_{ads} and $[C_{ad}^{*}+O_{ad}^{*}]$ and calculate the activation barrier of C-O bond dissociation on a γ-$Mo_2N(111)$ catalyst.

Calculation procedure

The $DMol^3$ module of Material Studio (version 6.0) from Accelrys Inc. (San Diego, CA, USA) was used to perform the DFT calculations. Accordingly, the electronic wave functions were expanded in numerical atomic basis sets defined on an atomic-centred spherical polar mesh. The double-numerical plus P-function (DNP) of all electron basis set, was used for all the calculations. The DNP basis set includes one numerical function for each occupied atomic orbital and a second set of functions for valence atomic orbitals, plus a polarization p-function on all atoms. Each basis function was restricted to a cut-off radius of 4.4 Å, allowing for efficient calculations without loss of accuracy. The Kohn-Sham equations [16] were solved by a self-consistent field procedure using PW91 functional with GGA for exchange correlation [17–19]. The techniques of direct inversion in an iterative subspace with a size value of six and thermal smearing of 0.005 Ha were applied to accelerate convergence. Optimization convergence thresholds for energy change, maximum force, and maximum displacement between the optimization cycles were set at 0.00002 Ha, 0.004 Ha/Å, and 0.005 Å, respectively. The k-point set of (1×1×1) was used for all calculations, which help to reduce the computation cost of this large slab/cluster arrangement. The activation energy of interaction between two surface species was identified by complete linear synchronous transit and quadratic synchronous transit search methods [20] followed by TS confirmation through the nudge elastic band method [21–23]. Spin polarization was imposed in all the calculations. The adsorption energy of an element (i.e. molecule or atom) was found according to the following formula:

$$E_{ad} = E_{\text{slab+element}} - \{E_{\text{empty slab}} + E_{\text{element}}\} .$$

Building unit cell structure of γ-Mo_2N crystal

γ-Mo_2N has a cubic B1 type crystal structure belonging to the $Fm\bar{3}m$ space group with lattice parameters a = b = c = 4.14613 Å. The unit cell of Mo_2N crystal was built following the atomic coordinate position (x, y, z); Mo at (0, 0, 0) and N at (0.5, 0.5, 0.5) according to experimental finding of Bull *et al.* [24]. The studied (111) plane was then cleaved from the unit cell. Further, the cleaved plane was increased to five atomic layers and 4×4 supercell, comprised of total 57 atoms, as shown in Fig. 1. The periodic supercell was converted into a non-periodic cluster. A larger surface area was generated to provide favourable adsorption locations for CO, C, and O species. The γ-$Mo_2N(111)$ plane has mainly four different adsorption sites, an on-top site, a bridge-bonding site between two Mo atoms and two threefold sites, with an underneath N atom (in 1st sublayer), a 3-fold hollow hcp site with an underneath Mo atom (2nd sublayer), and a 3-fold hollow fcc site. The underneath N atom layer is located very close to the top Mo layer, only at a 0.736-Å depth while the distance to the next Mo sublayer from the top surface is 2.081 Å, which suggests a pronounced electronic influence/contribution of Mo and N atoms to the top Mo layer. The distance between two surface Mo atoms is 2.942 Å and the angle between the Mo atoms is 60°. The charge on indexed Mo and N atoms of γ-$Mo_2N(111)$ (Fig. 1) are tabulated in Table 1.

RESULTS AND DISCUSSION

Adsorption and dissociation energies of CO over γ-$Mo_2N(111)$ plane

A DFT simulation was conducted for CO adsorption on four different adsorption locations over the γ-$Mo_2N(111)$plane, i.e. on-top, bridge-bonding, 3-fold hollow fcc, and 3-fold hollow hcp sites. Adsorption locations are depicted in Fig. 1 and adsorption arrangements and atomic distances from the surface plane are displayed in Table 2. Stable CO adsorption was found for all the above-mentioned arrangements. Carbon monoxide was molecularly adsorbed vertically having the 'C' end towards the surface for all the cases, which is common for non-dissociative CO chemisorption on most of the metal surfaces because the available electron donation orbital (5σ) is located on the carbon atom of the CO molecule, as explained by Blyholder [25]. Different adsorption arrangements of the CO molecule are explained below.

CO was adsorbed on a $Mo_{(4)}$ surface atom as on-top configuration. The obtained energy value of CO adsorption on the γ-$Mo_2N(111)$ plane as on-top arrangement was –30.87 kcal.mol^{-1} or –1.34 eV. The C-O bond length of non-dissociatively adsorbed CO was found to be equal to 1.185 Å. This length is greater than the molecular CO bond length of 1.14 Å. Therefore, CO adsorption on a γ-$Mo_2N(111)$ slab makes the C-O bond relaxed. The vibrational frequency of CO on the γ-$Mo_2N(111)$ plane was found to be 2663.06 cm^{-1}.

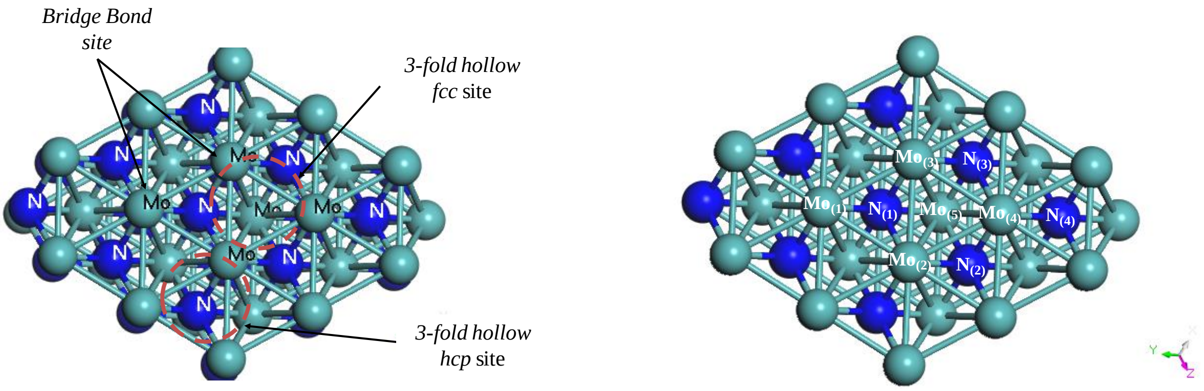

A γ-$Mo_2N(111)$ cluster showing different adsorption sites.

A γ-$Mo_2N(111)$ cluster with atomic indexing of neighbouring adsorption sites.

Fig. 1. γ-$Mo_2N(111)$ cluster top view.

Table 1. Atomic charge distribution over γ-$Mo_2N(111)$ with adsorbed species.

Atomic index*	Mulliken atomic charge, *e*									
	empty Mo_2N slab	on-top CO adsorption	bridge CO adsorption	CO adsorption on hcp site	CO adsorption on fcc site	carbon adsorption on fcc site	carbon adsorption on hcp site	oxygen adsorption on fcc site	oxygen adsorption on hcp site	carbon on fcc and oxygen on hcp site
$Mo_{(1)}$	0.561	0.563	0.623	0.633	0.567	0.579	0.666	0.563	0.737	0.772
$Mo_{(2)}$	0.545	0.569	0.584	0.609	0.633	0.676	0.642	0.751	0.711	0.849
$Mo_{(3)}$	0.545	0.573	0.586	0.609	0.633	0.677	0.614	0.751	0.711	0.668
$Mo_{(4)}$	0.496	0.457	0.572	0.508	0.581	0.626	0.524	0.701	0.500	0.632
$Mo_{(5)}$	0.951	0.948	0.948	0.949	0.941	0.941	0.949	0.941	0.951	0.937
$N_{(1)}$	–1.158	–1.158	–1.141	–1.126	–1.154	–1.15	–1.101	–1.155	–1.127	–1.149
$N_{(2)}$	–1.183	–1.187	–1.182	–1.182	–1.183	–1.186	–1.182	–1.193	–1.181	–1.186
$N_{(3)}$	–1.168	–1.168	–1.166	–1.169	–1.163	–1.158	–1.171	–1.165	–1.167	–1.157
$N_{(4)}$	–1.168	–1.17	–1.166	–1.169	–1.163	–1.159	–1.171	–1.165	–1.167	–1.169
C	0.105	0.068	–0.035	–0.089	–0.083	–0.420	–0.403	x	x	–0.575
O	–0.105	–0.186	–0.183	–0.180	–0.180	x	x	–0.595	–0.566	–0.411

* Atomic indices are according to Fig. 1

For a bridge-bonding configuration of CO, a simulation procedure was performed by binding CO to $Mo_{(2)}$ and $Mo_{(3)}$ surface atoms, where the carbon atom was bonded to two Mo atoms and the O atom remained on-top of the C atom as a linear arrangement. The adsorption energy of CO on a bridge-bonding site on the γ-$Mo_2N(111)$ plane was –33.22 kcal.mol^{-1} or –1.44 eV. The C-O bond length of non-dissociatively adsorbed CO was found to be equal to 1.209 Å, i.e. more relaxed compared to the on-top adsorption configuration. The vibrational frequency of CO for bridged adsorption was found to be 1769.07 cm^{-1}. For a 3-fold hollow hcp adsorbed configuration of CO, a simulation procedure was performed through bonding the CO to $Mo_{(1)}$, $Mo_{(2)}$, and $Mo_{(3)}$ surface atoms with an underneath $N_{(1)}$ atom, where the carbon atom was bonded to three Mo atoms and O remained on-top of the C atom as a linear arrangement. CO adsorption on a 3-fold hollow hcp site on the γ-$Mo_2N(111)$ plane gave an energy value of –34.34 kcal.mol^{-1} or –1.49 eV. The C-O bond length of non-dissociatively adsorbed CO was found to be equal to 1.217 Å, which is more relaxed compared to the on-top and bridging configurations. The vibrational frequency of CO for this adsorption arrangement was found to be 2194.47 cm^{-1}. Another simulation was performed for CO adsorption on a 3-fold hollow fcc site by bonding CO to $Mo_{(2)}$, $Mo_{(3)}$, and $Mo_{(4)}$ surface atoms with an underneath $Mo_{(5)}$ atom, where the carbon atom was bonded to three Mo atoms and O remained on-top of the C atom as a linear species. The energy value of CO adsorption on a 3-fold hollow fcc position on the γ-$Mo_2N(111)$ plane was –35.98 kcal.mol^{-1} or –1.56 eV. The C-O bond length of non-dissociatively adsorbed CO was found to be equal to 1.217 Å, which is more relaxed compared to the on-top and bridging configurations but similar to the 3-fold hollow hcp site. The vibrational frequency of CO for this arrangement was found to be 1844.45 cm^{-1}.

Among all adsorption modes, carbon monoxide was most strongly bonded at a 3-fold fcc position, which may be the preferred adsorption arrangement for CO on the γ-$Mo_2N(111)$ plane. Yang *et al.* [26] studied the vibrational frequency of CO on a fresh Mo_2N/Al_2O_3 catalyst. They assigned infrared bands at 2045 and 2200 cm^{-1} to CO adsorption onto 3-fold hollow hcp sites on the Mo_2N catalyst. This study also found a very close CO vibrational frequency, 2194.47 cm^{-1}, for a 3-fold hollow hcp adsorption arrangement but the adsorption energy was little less compared to the 3-fold hollow fcc configuration.

Molecular carbon monoxide adsorption values on the γ-$Mo_2N(111)$ plane have not been reported so far in the literature. Flapper *et al.* [27] stated an adsorption energy of –1.49 eV for CO adsorption on a 3-fold site of $Mo_2N(100)$ plane whereas Liu and Rodreguez [7] reported an adsorption energy value of –1.74 eV for on-top CO on a δ-MoN(001) plane.

Electronic charge distribution over the surface

Electronic charge distribution (Mulliken charge) values are given in Table 1 for the indexed Mo and N atoms of γ-$Mo_2N(111)$, atom indices are shown in Fig. 1, and for adsorbed C and O atoms. For an on-top adsorbed CO molecule on a $Mo_{(4)}$ atom, calculated values of Mullikan atomic charges on C and O were +0.068*e* and –0.186*e*, respectively. Atomic charges on C and O atoms of a free CO molecule are +0.105*e* and –0.105*e*, respectively. Reduced charges on C and O atoms indicate that a process of electron back donation from surface molybdenum atoms is taking place. The back donation of electron to the adsorbed CO molecule increases the antibonding orbital population and hence making the C-O bond weaker. At the same time the $Mo_{(4)}$ atom, to which CO was bonded, had a decrease in charge from +0.496*e* to +0.457*e* whereas other close surrounding surface $Mo_{(1,2,3)}$ atoms experienced an increase in their positive charge. Charges on underneath $Mo_{(5)}$ and $N_{(1,2,3,4)}$ atoms did not change to a considerable extent, suggesting their less involvement in electron donation/bonding process. Charge distribution results suggest that the electrons are drown from other nearby surface Mo atoms to the bonding Mo atom, i.e. $Mo_{(4)}$, and are back donated to CO, which makes the CO bond relaxed and reactive.

For bridge-bonded carbon monoxide on $Mo_{(2)}$ and $Mo_{(3)}$, the calculated values of Mullikan atomic charges of C and O were –0.035*e* and –0.183*e*, respectively, i.e. a decrease in charge value compared to on-top adsorption configuration. Charges on surface $Mo_{(1,2,3,4)}$ atoms were increased compared to the empty slab. The increase in charge was less for the $Mo_{(2)}$ and $Mo_{(3)}$ atoms and more for the $Mo_{(1)}$ and $Mo_{(4)}$ entities. Charges on the underneath $Mo_{(5)}$ and $N_{(1,2,3,4)}$ atoms were not changed to a considerable extent, suggesting less involvement in the electron donation/bonding process. Charge distribution results suggest that the electrons are drown from other surface atoms to the bonding atoms, $Mo_{(2)}$ and $Mo_{(3)}$, and are back donated to the carbon monoxide, which makes the CO bond more relaxed as indicated by the increase in C-O bond length.

For 3-fold hollow hcp adsorption of carbon monoxide on $Mo_{(1)}$, $Mo_{(2)}$, and $Mo_{(3)}$ atoms, calculated values of Mulliken atomic charges on C and O in the adsorbed CO molecule were –0.089*e* and –0.180*e*, which is a decrease in charge on the C and

O atoms compared to the bridge bonding configuration. Positive charges on the surface $Mo_{(1,2,3,4)}$ atoms were increased compared to the empty slab. The increase in charge was less for the $Mo_{(4)}$ atom compared to the $Mo_{(1)}$, $Mo_{(2)}$, and $Mo_{(3)}$ atoms to which the CO molecule was bonded. Interesting charge was decreased for the underneath $N_{(1)}$ atom from –1.158*e* to –1.126*e*, which signifies involvement of underneath N atom layer in charge donation and surface bonding process. Charges on underneath $Mo_{(5)}$ and $N_{(2,3,4)}$ atoms were not changed to a considerable extent, which implies less participation in electron donation/bonding process. Charge distribution results suggest that the electrons are drown from surface Mo atoms and underneath N atom and back-donated to CO, which makes the CO bond more relaxed as indicated by an increase of the C-O bond length compared to on-top and bridge bonding configurations.

Calculated values of Mulliken atomic charges on C and O atoms of CO molecule adsorbed on a 3-fold hollow fcc site on $Mo_{(2)}$, $Mo_{(3)}$, and $Mo_{(4)}$ atoms were –0.083*e* and –0.180*e*, respectively. Compared to a 3-fold hcp site the charge on the C atom was reduced, while that on the O atom remained the same. Positive charges on surface $Mo_{(1,2,3,4)}$ atoms were increased compared to the empty slab. The increase in charge was less for the $Mo_{(1)}$ atom compared to the $Mo_{(2)}$, $Mo_{(3)}$, and $Mo_{(4)}$ atoms. Charges on underneath $Mo_{(5)}$ and $N_{(1,2,3,4)}$ atoms changed to a little extent; there was a decrease of positive charge for the $Mo_{(5)}$ atom and all the underneath N atoms underwent a decrease in negative charge that indicated their contribution to electron donation and bonding. Charge distribution results suggest that electrons are drown from surface Mo atoms and underneath N and Mo atoms and are back donated to CO, which makes the CO bond more relaxed as indicated by an increase in CO bond length compared to on-top and bridge bonding sites.

Preferred adsorption location for C and O atoms over γ-Mo_2N(111)

Before calculating the dissociation energy barrier of CO, the preferred adsorption sites for atomic oxygen (O) and carbon (C) on the γ-Mo_2N(111) surface were performed by adsorbing C and O atoms separately on the surface and then place them together on the surface, thus building the preferred (lowest energy) surface product configuration of [C_{ad}+O_{ad}]. Table 2 shows adsorption arrangement for product configuration. For both C and O atoms, the preferred adsorption location was 3-fold hollow fcc and then 3-fold hollow hcp sites. On-top and bridge bonding adsorption configurations are not possible on γ-Mo_2N(111).

For a 3-fold hollow hcp adsorbed configuration of C atom, a simulation procedure was performed through bonding a C atom to $Mo_{(1)}$, $Mo_{(2)}$, and $Mo_{(3)}$ surface atoms with underneath $N_{(1)}$ atom. The obtained energy value of C atom adsorption on the γ-Mo_2N(111) plane was –65.45 kcal.mol^{-1} or –2.83 eV. Another simulation was carried out for bonding a C atom to $Mo_{(2)}$, $Mo_{(3)}$, and $Mo_{(4)}$ surface atoms with underneath $Mo_{(5)}$ atom on a 3-fold hollow fcc site. In this case the energy value of C atom adsorption on γ-Mo_2N(111) was –65.96 kcal.mol^{-1} or –2.86 eV. Therefore, a 3-fold hollow fcc site is more favourable for C atom adsorption than a 3-fold hollow hcp site. Similarly, for an O atom, a simulation was performed by bonding an O atom to $Mo_{(1)}$, $Mo_{(2)}$, and $Mo_{(3)}$ surface atoms with underneath $N_{(1)}$ atom for a 3-fold hollow hcp configuration. The found energy value of O atom adsorption on the γ-Mo_2N(111) plane was –63.35 kcal.mol^{-1} or –2.74 eV. Further, simulation of adsorbed O atom on a 3-fold hollow fcc site of $Mo_{(2)}$, $Mo_{(3)}$, and $Mo_{(4)}$ surface atoms with underneath $Mo_{(5)}$ atom was carried out. The adsorption value was –65.17 kcal.mol^{-1} or –2.82 eV. Therefore, a 3-fold hollow fcc site is also a favourable adsorption site for O atom.

Simultaneous adsorption of C and O atoms on their preferred locations on the γ-Mo_2N(111) plane, i.e. both a C atom and an O atom on a 3-fold hollow fcc site, was performed. The adsorption energy of atomic C and O over γ-Mo_2N(111) was –2.77 eV. The distance between the C and O species on the surface was 3.11 Å. Charge distribution showed that both the C and O atoms had a negative charge, –0.575*e* and –0.411*e*, respectively. It should be noted that non-bonded C and O have 0*e* charges. Positive charges on all the surface Mo atoms and underneath Mo atoms were increased (a 3-fold hollow fcc site has an underneath Mo atom) and for the underneath N atoms charges were not changed much. Therefore, the main contribution to bonding came from charge donation from surface Mo atoms.

Transition state search for CO dissociation

A transition state search was performed between a CO molecule adsorbed on a 3-fold hollow fcc site and a product configuration [C_{ad}+O_{ad}] adsorbed on two different 3-fold hollow fcc sites. A complete Linear Synchronous Transit/Quadratic Synchronous Transit (LST/QST) search was accomplished with a root mean square (RMS) convergence of 0.002 Ha/Å.

Table 2. Adsorption energies and surface adsorption arrangement and atomic distances of C and O atoms and CO molecule on γ-$Mo_2N(111)$ plane.

Adsorbed entity	Adsorption arrangement	Pictorial description	Adsorption energy eV	Atomic distance Å
CO	on-top adsorption on a Mo surface atom	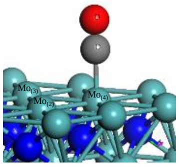	–1.34	$d_{C–O}$ = 1.185 $d_{Mo–C}$ = 2.121
CO	bridge site adsorption on two surface Mo atoms.	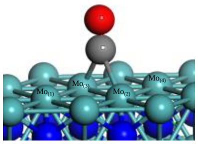	–1.44	$d_{C–O}$ = 1.209 $d_{Mo2–C}$ = 2.29 $d_{Mo3–C}$ = 2.29
CO	3-fold hcp site adsorption on three Mo atoms (underneath N atom)	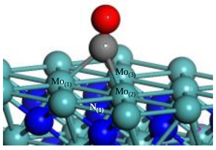	–1.49	$d_{C–O}$ = 1.217 $d_{Mo1–C}$ = 2.349 $d_{Mo2–C}$ = 2.370 $d_{Mo3–C}$ = 2.377
CO	3-fold fcc site adsorption on three Mo atoms (underneath Mo atom)	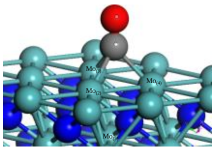	–1.56	$d_{C–O}$ = 1.217 $d_{Mo2–C}$ = 2.375 $d_{Mo3–C}$ = 2.372 $d_{Mo4–C}$ = 2.340
C atom	3-fold fcc site (underneath Mo atom)	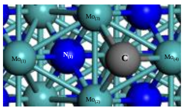	–2.86	$d_{Mo2–C}$ = 2.212 $d_{Mo3–C}$ = 2.214 $d_{Mo4–C}$ = 2.196
O atom	3-fold fcc site (underneath Mo atom)	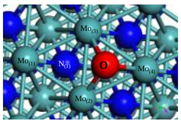	–2.83	$d_{Mo2–O}$ = 2.212 $d_{Mo3–O}$ = 2.214 $d_{Mo4–O}$ = 2.196
C and O atom	adsorption on two different 3-fold fcc sites (underneath Mo atom)	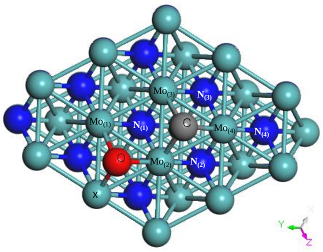	–2.77	$d_{C–O}$ = 3.119 $d_{Mo2–C}$ = 2.225 $d_{Mo3–C}$ = 2.204 $d_{Mo4–C}$ = 2.160 $d_{Mo1–O}$ = 2.195 $d_{Mo1–O}$ = 2.223 $d_{MoX–O}$ = 2.087

Dissociation activation barrier was found to be 67.96 kcal.mol^{-1} or 2.95 eV, while endothermic reaction energy was +28.87 kcal.mol^{-1}. The activation barrier of CO dissociation was quite large compared to carbon monoxide molecular adsorption energy, –35.98 kcal.mol^{-1} or –1.56 eV. So the DFT simulation suggests desorption of CO from the surface in molecular form rather than undergoing a CO dissociation step over the γ-$Mo_2N(111)$ plane. Fig. 2 depicts the transition state of CO dissociation reaction having the surface arrangement of CO at different NEB simulation points. C-O bond length was kept on increasing from 1.22 to 2.09 Å. A transition state search was also performed for a CO molecule adsorbed on a 3-fold hollow hcp site and [C_{ad}+O_{ad}] adsorbed on two different neighbouring 3-fold hollow fcc sites. The activation energy was little less compared to CO adsorbed on a 3-fold hollow fcc site as depicted in Fig. 3. Dissociation activation barrier was found 53.03 kcal.mol^{-1} or 2.30 eV whereas endothermic reaction energy was +27.13 kcal.mol^{-1}. The activation barrier for CO dissociation was still higher than the molecular CO adsorption energy suggesting the same conclusion that CO would prefer to desorb from the surface rather than undergo dissociation, as for the previous one.

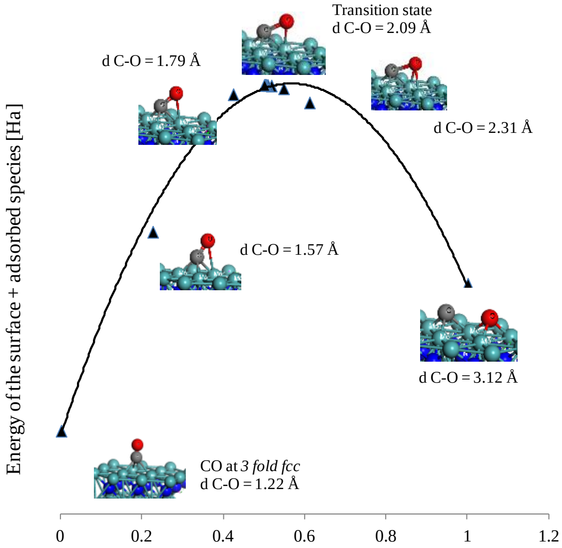

Fig. 2. Transition state search by NEB method for CO dissociation over γ-$Mo_2N(111)$ for CO adsorbed on a 3-fold fcc location.

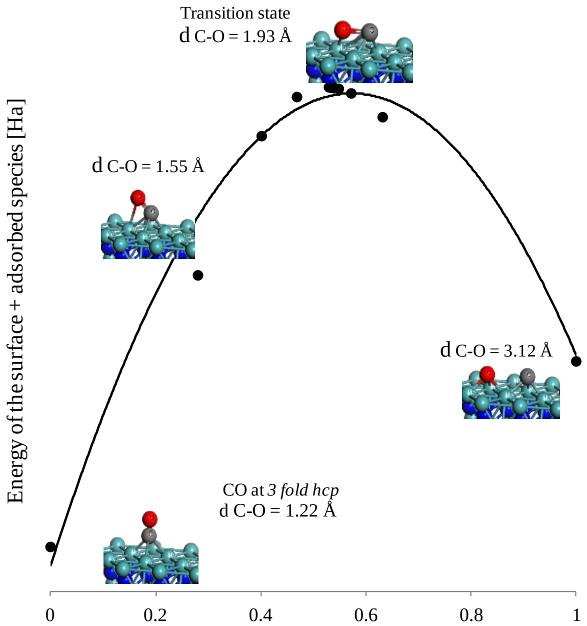

Fig. 3. Transition state search by NEB method for CO dissociation over γ-$Mo_2N(111)$ for CO adsorbed on a 3-fold hcp location.

Table 3 presents CO dissociation barrier and reaction energies on different molybdenum-based catalysts. Among reported catalysts, the activation barrier varies from low to high values in the following order: Mo_2C < MoS_2 ≤ Mo_2N < MoP. Close CO dissociation barrier values for MoS_2 and Mo_2N suggest similar surface reaction features for CO hydrogenation over these two catalysts.

Table 3. CO dissociation energies for Mo-based catalysts.

	Mo surface	Reaction energy, ΔE_r, kcal.mol^{-1}	Activation energy, ΔE_a, kcal.mol^{-1}	Ref.
$CO_{ad} \rightarrow [C_{ad}+O_{ad}]$	β-$Mo_2C(0001)$ Mo terminated	–21.91	20.52	[28]
	β-$Mo_2C(0001)$ C terminated	–5.99	44.28	[28]
	$MoS_2(10\bar{1}0)$ Mo edge	–3.23	59.96	[29]
	MoP(100)	62.49	87.17	[30]
	MoP(001)	–42.20	92.01	[31]
	γ-$Mo_2N(111)$	28.83	67.96	this work

CONCLUSIONS

Density functional theory (DFT) was employed to investigate carbon monoxide dissociation energy over γ-$Mo_2N(111)$ surface. Non-dissociative adsorption of CO on a 3-fold hollow fcc site was favoured on the surface with an adsorption energy of –35.98 kcal.mol^{-1}, while the adsorption energy for a 3-fold hollow hcp position was 34.34 kcal.mol^{-1}. Both the C and O atoms prefer a 3-fold hollow fcc bonding location. The dissociation activation energy barrier for CO adsorbed on a 3-fold hollow fcc position was 67.96 kcal.mol^{-1} while that for CO adsorbed on a 3-fold hollow hcp site was 53.03 kcal.mol^{-1}. Hence, the carbon monoxide molecule would prefer to desorb from the γ-$Mo_2N(111)$ surface rather than undergo dissociative adsorption.

Acknowledgement: This work was supported by the Deanship of Scientific Research (DSR), King Abdulaziz University, Jeddah, under grant No. (135-1013-D1435). The authors gratefully acknowledge the DSR technical and financial support.

REFERENCE

1. J. K. Nørskov, A. P. Frank, S. Felix, T. Bligaard (2010), PNAS early edition, www.pnas.org/cgi/doi/10.1073/pnas.1006652108 (2010).
2. S. A. Eliason, C. H. Bartholomew, *App. Catal. A-Gen.*, **186**, 229 (1999).
3. T. Bligaard, J. K. Norskov, S. Dahl, J. Matthiesen, C. H. Christensen, J. Sehested, *J. Catal.*, **224**, 206 (2004).
4. W. Ma, E. L. Kugler, J. Wright, D. B. Dadyburjor, *Energy Fuels*, **20**, 2299 (2006).
5. A. G. Constant, J.-M. Giraudon, G. Leclercq, L. Leclercq, *Appl. Catal. A-Gen.*, **260**, 35 (2004).
6. S. F. Zaman, K. J. Smith, *App. Catal. A-Gen.*, **378**, 59 (2010).

7. P. Liu, J. A. Rodriguez, *Catal. Lett.*, **91**, 247 (2003).
8. M. Huang, K. Cho, *J. Phys. Chem. C*, **113**, 5238 (2009).
9. X. R. Shi, J. Wang, K. Hermann, *J. Phys. Chem. C*, **114**, 13630 (2010).
10. J. G. Santiesteban, C. E. Bogdan, R. G. Herman, K. Klier, *Proc. 9th Int. Congr. Catal.*, **2**, 561 (1998).
11. M. Xiang, D. Li , H. Xiao, J. Zhang, H. Qi, W. Li, B. Zhong, Y. Sun, *Fuel*, **87**, 599 (2008).
12. G. Xie, T. Bai, L. An, H. Wang, J. You, *Reac. Kinet. Catal. Lett.*, **65**, 331 (1998).
13. C. Sepúlveda, K. Leiva, R. García, L. R. Radovic, I. T. Ghampson, W. J. DeSisto, J. L. García Fierro, N. Escalona, *Catal. Today*, **172**, 232 (2011).
14. S. Podila, S. F. Zaman, H. Driss, Y. A. Alhamed, A. A. Al-Zahrani, L. A. Petrov, *Catal. Sci. Technol.* DOI: 10.1039/C5CY00871A (2015).
15. S. Li, J. S. Lee, T. Hyeon, K. S. Suslick, *App. Catal. A-Gen.*, **184**, 1 (1999).
16. W. Kohn, L. J. Sham, *Phys. Rev.*, **140**, 1133 (1965).
17. J. P. Perdew, J. A. Chevary, S. H. Vosko, K. A. Jackson, M. R. Pederson, D. J. Singh, C. Fiolhais, *Phys. Rev. B*, **46**, 6671 (1992).
18. A. D. Becke, *J. Chem. Phys.*, **88**, 2547 (1988).
19. J. P. Perdew, Y. Wang, *Phys. Rev. B*, **45**, 13244 (1992).
20. T. A. Halgren, W. N. Lipscomb, *Chem. Phys. Lett.*, **49**, 225(1997).
21. S. Bell, J. S. Crighton, *J. Chem. Phys.*, **80**, 2464 (1983).
22. S. Fischer, M. Karplus, *Chem. Phys. Lett.*, **194**, 252 (1992).
23. G. Henkelman, H. Jónsson, *J. Chem. Phys.*, **113**, 9978 (2000).
24. C. L. Bull, T. Kawashima, P. F. McMillan, D. Machon, O. Shebanova, D. Daisenberger, E. Soignard, E. T. Muromachi, L. C. Chapon, *J. Solid State Chem.*, **179**, 1762 (2006).
25. G. Blyholder, *J. Phys. Chem.*, **68**, 2772 (1964).
26. S. Yang, C. Li, J. Xu, Q. Xin, *Chem. Commun.*, 1247 (1997).
27. G. Frapper, M. Pélissier, J. Hafner, *J. Phys. Chem. B*, **104**, 11972 (2000).
28. X. Shi, J. Wang, K. Hermann, *J. Phys. Chem. C*, **114**, 13630 (2010).
29. M. Huang, K. Cho, *J. Phys. Chem. C*, **113**, 5238 (2009).
30. S. F. Zaman, M. Daous, L. Petrov, *C. R. Acad. Bulg. Sci.*, **66**, 1083 (2013).
31. S. F. Zaman, M. Daous, L. Petrov, *C. R. Acad. Bulg. Sci.*, **67**, 1535 (2014).

ИЗСЛЕДВАНЕ С ТФП НА АДСОРБЦИЯТА И ДИСОЦИАЦИЯТА НА CO ВЪРХУ γ-Mo$_2$N(111) КРИСТАЛНА РАВНИНА

Ш. Ф. Заман

Департамент по инженерна химия и материали, Факултет по инженерство, Университет Крал Абдулазис, п.к. 80204, Джеда 21589, Саудитска Арабия
Катедра „Катализ“ на Саудитската основна индустриална корпорация, Департамент по инженерна химия и материали, Факултет по инженерство, Университет Крал Абдулазис, п.к. 80204, Джеда 21589, Саудитска Арабия

Постъпила на 9 октомври 2015 г.; Преработена на 23 ноември 2015 г.

(Резюме)

Проведено е теоретично изследване с теорията на функционала на плътността на енергетичната бариера на дисоциацията на въглероден оксид върху кристалната равнина γ-Mo$_2$N(111). Дисоциацията на CO е ендотермична реакция с топлинен ефект 28.87 kcal.mol^{-1} и висока енергетична бариера от 67.96 kcal.mol^{-1}, започваща с молекулна адсорбция на CO на трицентрови места със стенно центрирана кубична плътна опаковка с енергия на адсорбция 35.98 kcal.mol^{-1}. Енергетичната бариера е по-ниска, 53.03 kcal.mol^{-1}, когато молекулната адсорбция на CO е върху трицентрови места с хексагонална плътна опаковка с енергия на адсорбция 34.34 kcal.mol^{-1}. И в двата случая процесът на дисоциация на CO е кинетически ограничен. Наблюдава се съществен електронен ефект на азотния лиганд и на молибдена от лежащия отдолу слой при образуване на връзки в адсорбционния слой на повърхността.